Attention Augmented ConvNeXt UNet For Rectal Tumour Segmentation

Hongwei Wu ; Junlin Wang *; Xin Wang *;Hui Nan ; Yaxin Wang ; Haonan Jing ;Kaixuan Shi

ABSTRACT

It is a challenge to segment the location and size of rectal cancer tumours through deep learning. In this paper, in order to improve the ability of extracting sufficient feature information in rectal tumour segmentation, attention enlarged ConvNeXt UNet (AACN-UNet), is proposed. The network mainly includes two improvements: 1) the encoder stage of UNet is changed to ConvNeXt structure for encoding operation, which can not only integrate multi-scale semantic information on a large scale, but also reduce information loss and extract more feature information from CT images; 2) CBAM attention mechanism is added to improve the connection of each feature in channel and space, which is conducive to extracting the effective feature of the target and improving the segmentation accuracy.The experiment with UNet and its variant network shows that AACN-UNet is 0.9% ,1.1% and 1.4% higher than the current best results in P, F1 and Miou.Compared with the training time, the number of parameters in UNet network is less. This shows that our proposed AACN-UNet has achieved excellent results in CT image segmentation of rectal cancer.

Keywords: UNet; Rectal Tumour Segmentation; Attention; Convolutional neural network

1.Introduction

Rectal cancer refers to the cancer from the dentate line to the junction of rectum and sigmoid colon, and is one of the most common malignant tumours of the digestive tract. [泰迪杯]. http://www.tipdm.org/u/cms/www/201903/.According to the cancer statistics of the United States in 2020. Rectal cancer is the second largest cancer threatening human health, with a large number of patients and a high mortality rate (Siegel et al. 2020). The occurrence and development of rectal cancer mostly follow the "adenoma cancer" sequence, and it generally takes 5-10 years to progress from precancerous lesions to cancer, which provides an important time window for early diagnosis and clinical intervention (Guideline…2020). In addition, the prognosis survival rate of rectal cancer is closely related to the prognosis and diagnosis stage of rectal cancer. The 5-year relative survival rate of stage I rectal cancer is 90.3%, while the 5-year relative survival rate of stage IV rectal cancer with distal metastasis is only 12.5% (Desantis et al. 2013). A large number of studies and practices show that early screening of rectal cancer through medical means can effectively reduce the mortality rate of rectal cancer (Green et al. 2018). In the 2021 edition of CSCO colorectal cancer diagnosis and treatment guide, enterostomy is listed as the gold standard for rectal cancer screening. However, enteroscopy has certain limitations. In addition to the high degree of pain during examination, it may also cause complications such as intestinal perforation, intestinal hemorrhage, mesenteric laceration, and cardiovascular and cerebrovascular accidents. In the 2021 edition of CSCO colorectal cancer diagnosis and treatment guide, the addition of "CT imaging examination" for individuals with contraindications to enteroscopy is rec-

ommended as level III. Due to the limitations of technology and the characteristics of rectal tumour itself, it is not obvious on CT images. If doctors work too much, rectal tumour may be neglected and misdiagnosed. Rectal tumour segmentation can assist doctors in diagnosis, reduce doctors' labor intensity, treat patients in time and save valuable time.

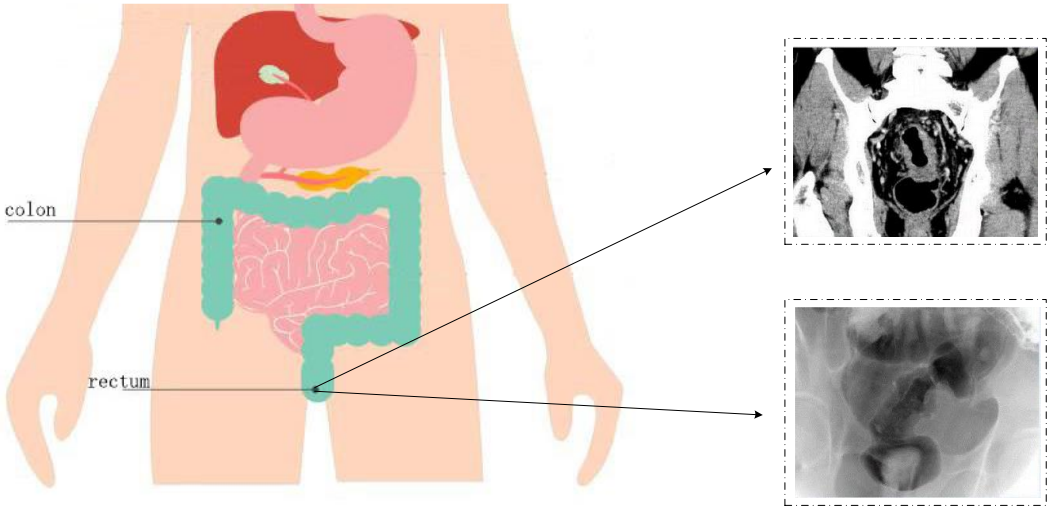

Figure 1 Rectal cancer tumor

Artificial intelligence (AI) is a hot topic in the academic and industrial circles. The problem of medical image segmentation through artificial intelligence can be traced back to the 1970s. The early medical image segmentation methods usually rely on edge detection, template matching technology, statistical shape model, active contour and machine learning. These technologies are applied to the detection of brain CT and lung CT. Although UNet, Attention-UNet and Transunet models have achieved good segmentation results in medical image segmentation, due to the particularity of rectal tumours, the CT images of rectal tumours often contain noise such as feces. In addition, it

is necessary to judge whether the intestinal cavity is eccentric and whether there is irregular thickening and other imaging characteristics. When these models are directly used in rectal tumour segmentation, although the segmentation of rectal tumours can be realized, the segmentation accuracy is not excellent.

Therefore, this paper proposes a new model called Attention Augmented ConvNeXt UNet (AACN-UNet), to explore more effective semantic information from a comprehensive scope. This paper refers to the U-shaped structure of UNet model to achieve feature fusion of multi-scale information. The model uses ConvNeXt as the backbone feature extraction network for coding operations. It can not only integrate multi-scale semantic information on a large scale, but also integrate sufficient fine and coarse grained semantic information in the decoding stage, so as to avoid information loss caused by compressed dimensions when information is converted between feature spaces of different dimensions, and achieve better results with fewer parameters, CBAM attention mechanism is used in the encoder and decoder paths to improve the relationship between each feature in the channel and space, which is more conducive to extracting effective features of the target. After the experimental verification of rectal cancer tumour segmentation, the use of ConvNeXt as the backbone feature extraction network and the U-shaped model with CBAM attention mechanism, compared with the UNet model, has fewer parameters, shorter training time, higher accuracy, and achieved excellent results.

The structure of this paper is as follows. The second section briefly summarizes the relevant research work. The third section introduces the AACN-UNet model. The

fourth section introduces the experimental setup, the description of the data set used, and the experimental process. Section fifth draws conclusions.

2.Related Works

In recent years, with the continuous improvement of computer hardware and software performance, deep learning algorithms have been more widely used. Researchers have put forward many effective algorithms. The UNet network model adopted the encoder and decoder structure (Ronneberger et al. 2015). The encoder part extracted image level features through convolution and step-by-step downsampling to encode the input image. The decoder mapped the coded signal into the corresponding binary segmentation mask through convolution and progressive upsampling to obtain the segmentation result. Inspired by the UNet model, many researchers have improved the UNet network. UNet++ model (Zhou et al. 2017), a set of partition architecture based on nested dense jump connection is proposed.The R2UNet model (Alom et al. 2018) adds the recurrent conv module on the basis of UNet to improve UNet; In Channel-UNet(Chen et al. 2019), UNet is the main structure of the network, and spatial channel convolution is added in each upsampling and downsampling module. Attention-UNet integrates attention mechanism into UNet model (Oktay et al. 2018).

Transformer architecture (Vaswani et al. 2017) has completely changed the field of Natural Language Processing (NLP) and migrated to the field of computer vision. However, due to the high demand for data, it also faces great challenges in medical image segmentation. Under the influence of transformer, the authors in Transunet can use transformers as a powerful encoder for medical image segmentation tasks through the

combination of transformer and UNet and by recovering local spatial information (Chen et al. 2021), and have achieved excellent performance in the field of multi organ segmentation. Swin-transformer proposes the method of moving windows to calculate self-attention in the non overlapping window area (Liu et al. 2021), and introduces the hierarchical construction method commonly used in CNN to build a hierarchical transformer. Swin-UNet uses the Swin-transformer structure as both an encoder and a decoder (Cao et al. 2021). While retaining the U-shaped structure and the deep neural network structure of jump connection, it also gives full play to the advantages of extracting multi-scale features and global and remote semantic information interaction in Swin-transformer, and has excellent effects in medical image segmentation.

Some people have proposed a convolutional neural network model for the 2020s ConvNeXt network (Liu et al. 2022). The author uses the ideas of Swin-transformer (Cao et al. 2021),ResNeXt (Xie et al. 2016) and Mobilenet (Howard et al. 2017) to change the calculation amount in different stages at the macro level, convolution with large-scale convolution kernel, group convolution, etc. In the micro design, the Relu activation function is replaced by Gelu activation function, fewer activation functions and normalization layers are used, and BN is replaced by LN. The network outperforms the Swin-t model in many classification tasks and recognition tasks to achieve the best performance.

In document Attention-UNet (Oktay et al. 2018), in order to suppress irrelevant areas in the input image and highlight the salient features of specific local areas, attention is integrated into the jump connection and upsampling module of UNet to realize

the spatial attention mechanism. In the semantic segmentation based on UNet, the combination of the low resolution information obtained by the encoder and the high-resolution information on the same height decoder can be better applied to medical images with fuzzy boundaries and complex gradients. However, this method treats each channel of the output features equally, so it lacks the flexibility to process the characterization information of different channels. SENet proposed a channel based attention model (Jie et al. 2017), which models the importance of each feature channel, and then enhances or suppresses different channels for different tasks. SKNet proposed an attention mechanism based on convolution kernel (Li et al. 2019), that is the importance of convolution kernel, the different images can get convolution kernels with different importance. After the spatial domain attention mechanism and the channel domain attention mechanism, someone proposed the CBAM attention mechanism (Sanghyun et al. 2018), which can focus on the important features of the image, suppress unnecessary regional responses, and realize the combination of the attention mechanism in the channel dimension and the spatial dimension. In the hybrid attention mechanism proposed by DANet (Fu et al. 2018), the positional attention mechanism is responsible for capturing the spatial dependence of the feature map at any two positions. Similar features will be related to each other regardless of the distance. The channel attention mechanism is responsible for integrating the relevant features of all channel maps to selectively emphasize the existence of interdependent channel maps

3. Method

This section introduces the basic structure of AACN-UNet and the CBAM attention module.

3.1 AACN-UNet structure

The basic structure of AACN-UNet is shown in Figure 1. It is mainly composed of the left contraction path and the right expansion path. The left side is the downsampling part and the right side is the upsampling part. In the down sampling part, ConvNeXt network is used as the backbone feature extraction network, and a stem operation is performed before entering ConvNeXt. Starting from vit, in order to convert the picture into a token, the picture will be divided into patches one by one. In the traditional ResNet, the stem layer uses a 7x7 convolution with stride = 2 and a maximum pooling layer. ConvNeXt imitates the practice of Swin-transformer and uses 4x4 convolution with stride = 4 to perform stem, so that the sliding windows do not intersect and only process the information of one patch at a time. Such processing has a good effect on extracting coarse-scale semantic information in rectal cancer CT images.

In the upsampling process, the double line upsampling method is used instead of the original deconvolution process to reduce the shadow problem in the original deconvolution process Then, each upsampling feature map is jump connected with the feature map obtained by the encoder. The introduction of jump connection can more highlight the foreground target and minimize the noise response generated when the feature fusion

is performed on the number of channels.

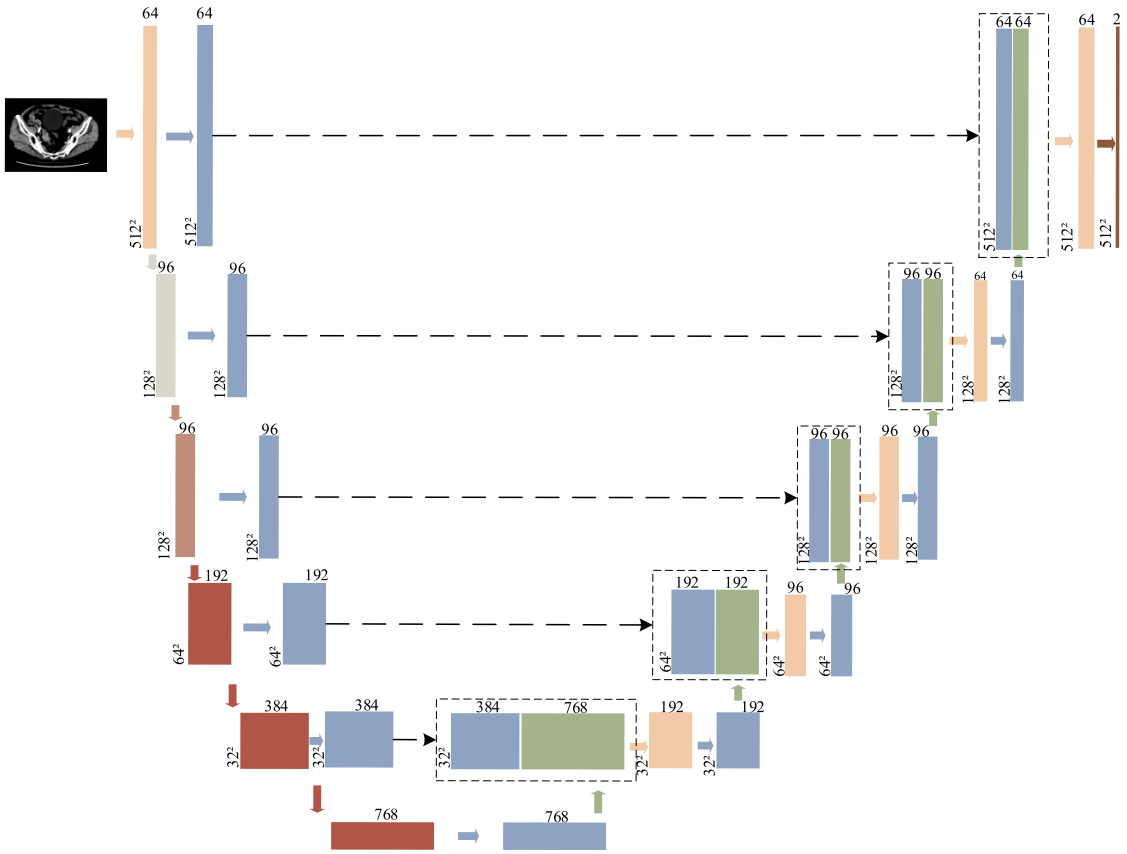

Figure 2. The gray arrow is the stem layer, it includes a 4x4 convolution with stride = 4 and a layer norm layer; Green arrow are bilinear upsampling; The blue arrow is the attention mechanism of CBAM; The orange arrow is the 4x4 convolution operation of twice stride = 1 and the relu operation; The red and brown arrow are separate ConvNeXt blocks, and the red arrow are dowmsample and ConvNeXt blocks; The point rectangle is a feature series, and the point arrow is a skip connection; The brown arrow in the last layer of the model is a convolution operation with kernel = 1×1.

The following figure shows ConvNeXt Block and Downsample.

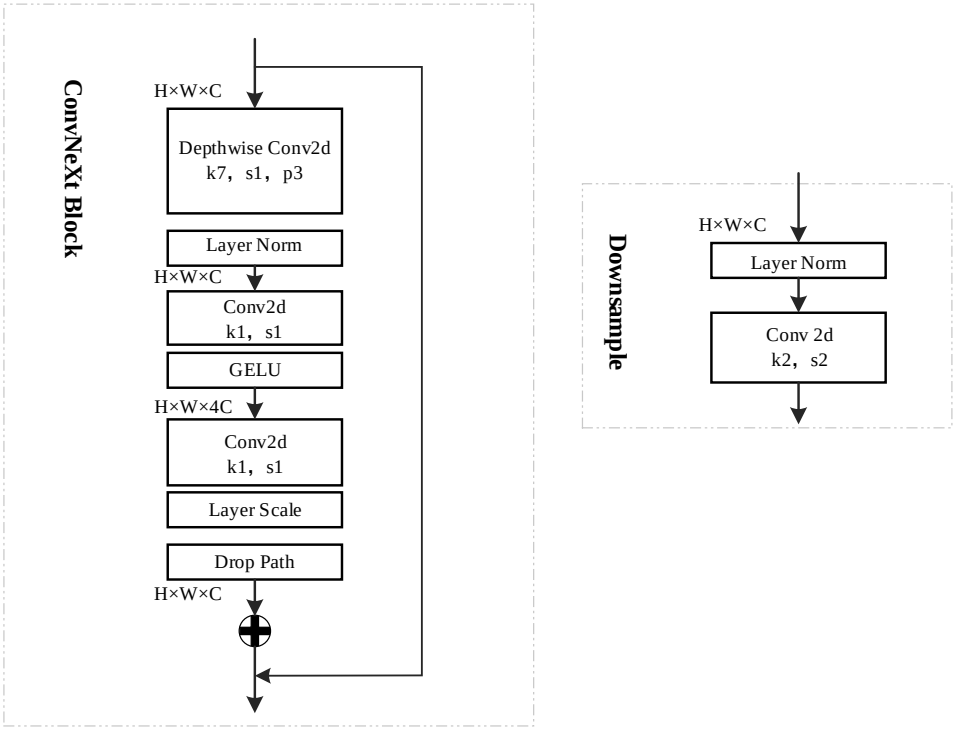

Figure 3.The ConvNeXt block adopts the form of small dimension, large dimension and small dimension to avoid the information loss caused by the compressed dimension when the information is converted between the feature spaces of different dimensions. The information is convoluted by a group with kernel = 7, stride = 1 and padding = 3, which can obtain better results with fewer parameters. Downsample is composed of a layer norm layer and a convolution with a convolution kernel=2 and stride= 2.

3.2CBAM attention module

For rectal cancer detection tasks. In this paper, CBAM composed of channel attention module (CAM) and spatial attention module (SAM) is integrated into the encoder and decoder path of the model As shown in Figure 3 and 4 below, it is the attention mechanism module of CBAM.

For the feature map generated by the network backbone, CBAM generates one-dimensional channel attention feature map and two-dimensional spatial attention feature map respectively:

$$F \in R^{C \times H \times W} \tag{1}$$

One-dimensional channel attention feature map:

$$M_c \in R^{C \times 1 \times 1} \tag{2}$$

Two-dimensional spatial attention feature map:

$$M_s \in R^{1 \times H \times W} \tag{3}$$

This process can be described as the following formula:

$$F' = M_C(F) \otimes F \tag{4}$$

$$F'' = M_s(F') \otimes F' \tag{5}$$

$\otimes$ represents element multiplication, in the middle, broadcast mechanism is used for dimension transformation and matching

The following figure 4 shows the channel attention mechanism

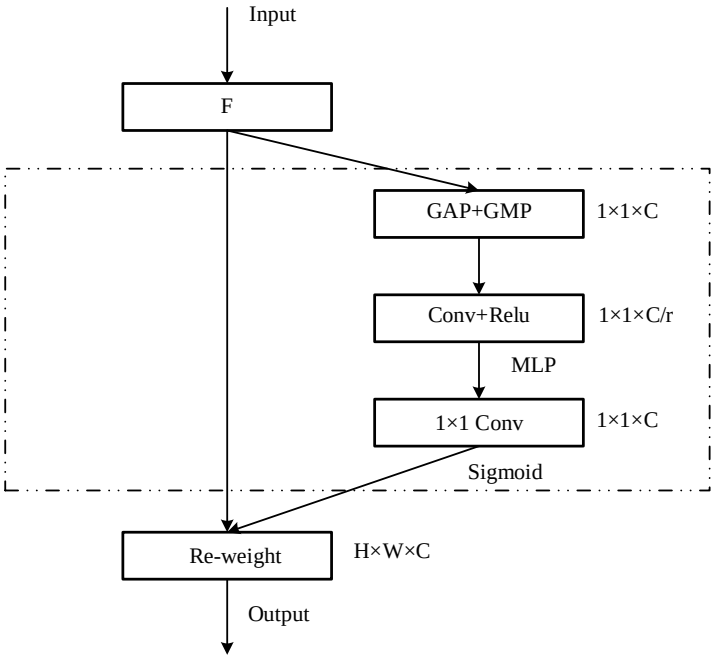

Figure 4.The channel attention mechanism

In order to better calculate the attention characteristics of the channel, after the input of the feature map, what we need to do is to compress the spatial dimension of the feature map, perform Global average pooling (GAP) and global max pooling (GMP) based on the width and height of the feature map, and then obtain the attention weight of the channel through MLP. To reduce the computational parameters, a dimension reduction coefficient r was used in MLP.

$$M_c \in R^{C/r\times 1\times 1} \tag{6}$$

Then, the normalized attention weight is obtained by sigmoid function. Finally, the channel attention is weighted to the original input feature map one by one by multiplication to complete the recalibration of the original feature. The formula is as follows, $F_{avg,}^{c} F_{max}^{c}$ represent the average pooling characteristics and the maximum pooling characteristics, respectively.

$$M_c(F) = \sigma\big(MLP\big(AvgPool(F)\big) + MLP(MaxPool(F))\big)$$

$$= \sigma(W_1\left(W_0\big(F_{avg}^c\big)\right) + W_1\big(W_0(F_{max}^c)\big) \quad (7)$$

The following figure 5 shows the spatial attention module

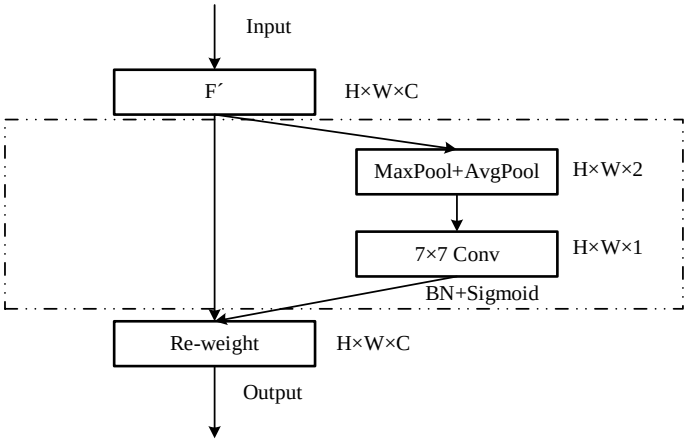

Figure 5.The spatial attention mechanism

In order to obtain the attention features in the spatial dimension, the feature maps generated by them are first concatenated. Then on the stitched feature map, convolution operation is used to generate the final spatial attention feature map. The formula is as follows, $F_{avg,}^s F_{max}^s$ is two dimensional feature maps generated using two pooling methods

$$M_s(F) = \sigma\big(f^{7\times7}\big((AvgPool(F)\big); (MaxPool(F))\big) = \sigma\left(f^{7\times7}\big(F_{avg}^s; F_{max}^s\big)\right) \quad (8)$$

In the spatial attention module, the global average pooling and maximum pooling obtain the spatial attention features, and the correlation between the spatial features is established through two convolutions, while the input and output dimensions are kept unchanged. By convolution operation (kernel = 7×7), the parameters and calculation amount are greatly reduced, which is conducive to establishing high-dimensional spatial

feature correlation. After CBAM, the new feature map will obtain the attention weight in the channel and space dimensions, which greatly improves the relationship between each feature in the channel and space, and is more conducive to extracting the effective features of the target.

In the encoder path, CBAM is combined into each layer of ConvNeXt to extract the feature layer part, and in the decoder part, it is placed after all the convolution layers (Figure 2), and the feature of the next level is used to supervise the feature of the upper level to realize the attention mechanism (restrict the active part to the area to be segmented, reduce the activation value of the background to optimize the segmentation, and realize end-to-end segmentation). This enables the model to perform channel and spatial attention, so it can better explore the relationship between channels and spaces of features.

2.3 Loss function

The purpose of model training is to obtain the optimal parameter set that can make the predicted label output of the model closest to the real label. Cross entropy is used to measure the similarity between the real label and the predicted label. The smaller the cross entropy of real tags and predicted tags, the higher the similarity between them, and the better the segmentation performance of the model.

CE loss (cross entropy loss) is the cross entropy loss function (Zhang et al. 2018), which is calculated by comparing the pixel level errors of prediction and label. The expression is as follows, where p is the real mark of the image, representing the probability of correct prediction in the image.

$$\text{loss} = -[\text{y} \cdot \log(\text{p}) + (1 - \text{y}) \cdot \log(1 - \text{p})] = \begin{cases} -\log(\text{P}) & \text{y} = 1 \\ -\log(1 - \text{P}) & \text{y} = 0 \end{cases} \quad (9)$$

Let *i* be the sample, and N represents the total number of samples, then the average cross entropy of the whole graph is shown in the formula

$$loss = -\frac{1}{N}\sum_{i=1}^{N}[y \cdot \log(p) + (1 - y) \cdot \log(1 - p)] \quad (10)$$

Dice loss takes the evaluation index of semantic segmentation as loss (Yeung et al. 2021). Dice coefficient is a set similarity measurement function, which is usually used to calculate the similarity between two samples, and the value range is [0,1].

The calculation formula is as follows:

$$Dice = \frac{2|X \cap Y|}{|X| + |Y|} \quad (11)$$

The calculation formula of dice loss is as follows

$$dice\ loss = 1 - Dice \quad (12)$$

Where X represents the predicted image and Y represents the real image.

The design of loss function needs to consider the characteristics of data sets. Due to the particularity of medical images, medical image slices may have the characteristics of fuzzy boundaries, low contrast and small targets. Using common loss functions, the convergence speed is slow and the learning effect is poor. Most loss functions designed for unbalanced data sets can solve the mild imbalance problem well. However, when the proportion of positive and negative samples is seriously unbalanced, the Dice coefficient appears more robust.

Therefore, the cross entropy loss function and dice loss function are used as the loss function in this paper.

$$loss = CE\ loss + dice\ loss \tag{13}$$

4. Experiment

In this section, a series of experiments were conducted to demonstrate the effectiveness of the proposed AACN-UNet network, all of which were conducted on the data set described below.

4.1 Data set acquisition

The data set used in this paper consists of the CT image data of 33 postoperative rectal cancer patients collected by Beijing anorectal association from 2015 to 2020 and the venous CT image data of 101 rectal cancer patients in the 7th Teddy cup data mining challenge in China [accessed 2022 Apr].http://www.tipdm.org/u/cms/www/201903/.The acquisition of the image data of the former was approved by the Ethics Committee of Beijing Anorectal Association, and the patient information was completely confidential. The latter is a marked public data set. The former is marked according to postoperative pathological sections and examination reports. Four imaging experts are invited to mark it, and the marking format is consistent with the former. In order to ensure the accuracy of labeling, all 4 experts participated in the labeling of 33 patients, and finally compared the labeling results and relabeled the samples in question.

There were 1794 positive (with lesions) samples in the data set, and each image contained a rectal cancer tumour area. In order to make the training accurate, 2-3 nega-

tive (no focus) CT images were introduced for each patient, a total of 506. 100 test sets were divided, including 94 positive samples and 6 negative samples. The remaining 2200 pieces are divided according to the proportion of training set: verification set =9:1

Due to the limitation of data resources and the small amount of data, this paper expands the data set. The main methods include randomly rotating the image within the range of - 180 ° - 180 °, horizontally turning and vertically turning the image, randomly cutting the image and restoring the original size, adjusting the image contrast, and adjusting the brightness and saturation. Figure 6 (a) after data expansion, the three original images are shown in figure (b) (c) (d) (e) (f) (g)

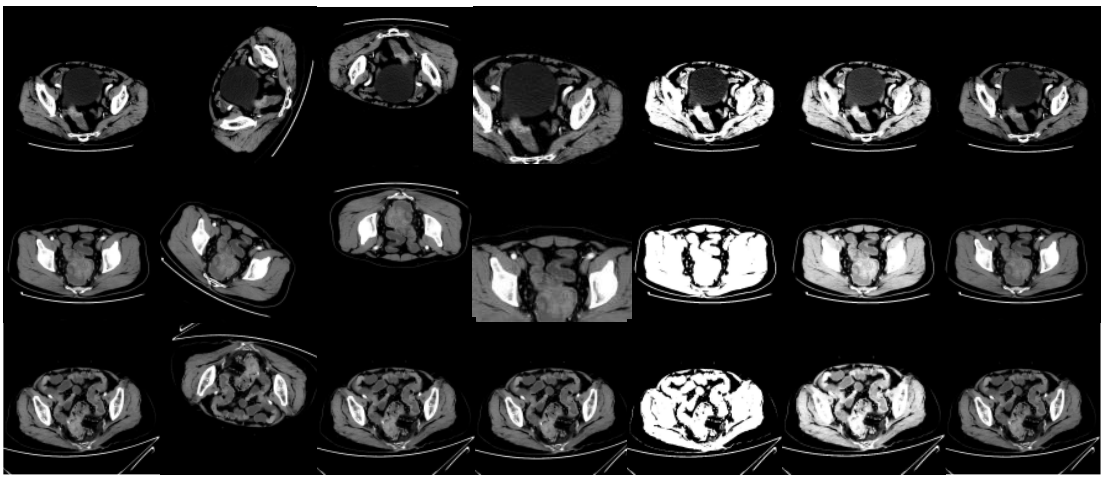

(a)Original drawing (b)Rotate (c)Flip (d)Crop (e)Contrast (f)Brightness (g)Saturation

Figure 6 Data expansion rendering

4.2 Performance Index

In order to verify the effectiveness of this method, the confusion matrix is used to evaluate the performance of the model based on the comparison of prediction graph and label graph Confusion matrix is a method to distinguish true positive (TP), true negative (TN), false positive (FP) and false negative (FN). Table 1 shows the construction method of confusion matrix. The actual value is shown in the list, the predicted value is

shown in the row.Four evaluation indexes were applied in the comparative experiment, namely, Miou, recall (R), precision (P), F-score.

Table 1.The construction method of confusion matrix in this experiment

Confusion matrix		Authentic label	
		Have tumour	No tumour
Prediction results	Have tumour	TP	FP
	No tumour	FN	TN

Iou is a standard measure of algorithm accuracy in image segmentation. The larger the Miou value, the higher the segmentation accuracy. The method of calculating Iou is to divide the intersection of the predicted area and the actual area by the union of the predicted area and the actual area, that is

$$IOU = \frac{A \cap B}{A \cup B} = \frac{TP}{TP+FP+FN} \tag{14}$$

The proportion of the part whose accuracy is positive and indeed positive in all classifiers that is considered to be positive indicates the proportion of the true prediction of the model in all positive example results in the prediction graph, that is

$$P = \frac{TP}{TP+FP} \tag{15}$$

Recall rate refers to the proportion of the part that the classifier considers to be a positive class and is indeed a positive class in all classifiers. It indicates the proportion that the model predicts correctly in all the results that the real value is a positive example, that is

$$R = \frac{TP}{TP+FN} \tag{16}$$

The evaluation index is for the sample label, and the evaluation model has the ability to recognize positive examples.

F1 value combines accuracy and recall, i.e

$$F1 = \frac{2 \times P \times R}{P+R} \tag{17}$$

The value range is 0~1, 1 represents the best output of the model, and 0 represents the worst output of the model

4.3 Experiment and Result Analysis

This article uses Python language design, based on pytorch deep learning framework. The hardware configuration of the operating platform is NVIDIA geforce rtx3090 super GPU with 24 GB video memory 15 core AMD epyc 7543 32 core processor CPU with 80g memory.

In this paper, the maximum number of iterations is set to 100, and the idea of literature (Trebing et al. 2021) is followed. The early stop criterion method is adopted to improve the training efficiency and avoid over fitting. In this case, if the verification set loss has not increased in the past 20 periods, the training is stopped. In order to initialize the learning rate, a series of values, namely 0.01, 0.005, 0.001, 0.0005 and 0.0001, were tested. According to the experiment, 0.001 is the best choice to set the initial learning rate. In terms of optimizer selection, this paper chooses to use Adam optimizer. After 5 steps, the learning rate is adjusted to the original 0.96, and the size of bathsize is set to 16. In the ConvNeXt backbone feature extraction network, the number of ConvNeXt

blocks at each layer is set to be the same as ConvNeXt-t, which are 3, 3, 9 and 3 respectively.

The comparative experimental results of eight rectal tumour segmentation networks are shown in Table 2. It is obvious that the performance of AACN-UNet is superior to other comparison networks in all four indicators, and the segmentation performance has been significantly improved. Compared with UNet, AACN-UNet has increased Iou, Pand F1 by 1.4%, 0.9% and 1.1% respectively, which is the best among other comparison networks. This shows that AACN-UNet has the best performance in rectal cancer tumour segmentation

Table 2.Segmentation results of different networks for rectal cancer

Module	P	R	F-Score	Iou
UNet	94.1	95.2	94.0	90.1
Resnet50-UNet	92.5	91.4	92.2	86.8
UNet++	93.8	92.6	93.4	88.3
Channel UNet	86	**97.2**	87.7	84.8
Attention-UNet	86.2	96.8	87.9	84.8
R2UNet	87.7	82.3	84.4	75.8
Transunet	88.4	95.1	89.3	85.4
AACN-UNet	**95**	95.3	**95.1**	**91.5**

It can be seen from the above table that both UNet and AACN-UNet have achieved excellent results in rectal cancer tumour segmentation.

The following table shows the comparison of parameters between UNet and AACN-UNet. The total params,params size and training time of AACN-UNet are lower than those of UNet.

Table 3. Number of network parameters and training time.

Parameter comparison		Number of parameters		training time（hour）
		Total params（MB）	Params size（MB）	
Network model	UNet	4.39	167.59	12.68
	AACN-UNet	3.13	119.44	11.617

The figure below shows the comparison between the parameters and inference time of the eight networks. In the figure, the inference speed of Transunet is also extremely fast when the parameters are small. The AACN-UNet designed in this paper also shows good performance.

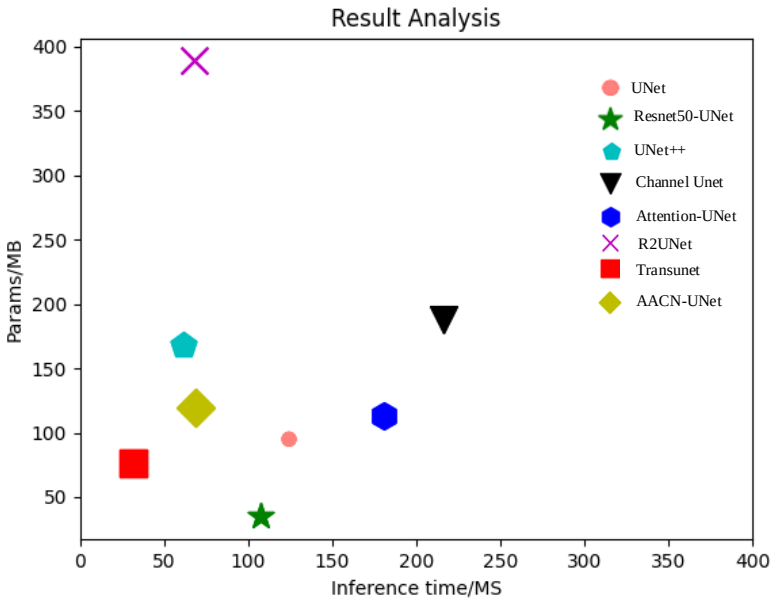

Figure 7 Model result analysis

The following figure shows the segmented images obtained by predicting the weights of five CT images in the test set after the training of the above eight models. The first column is the original CT image, the second column is the real image, and the

segmentation results are from the third column to the eighth column. Obviously, the segmentation results of AACN-UNet are mostly similar to real label images, and the dice values listed at the bottom of each segmented image also support this conclusion. Although AACN-UNet achieves the most advanced segmentation performance, it is unknown whether the addition of CBAM attention mechanism improves the performance of the model

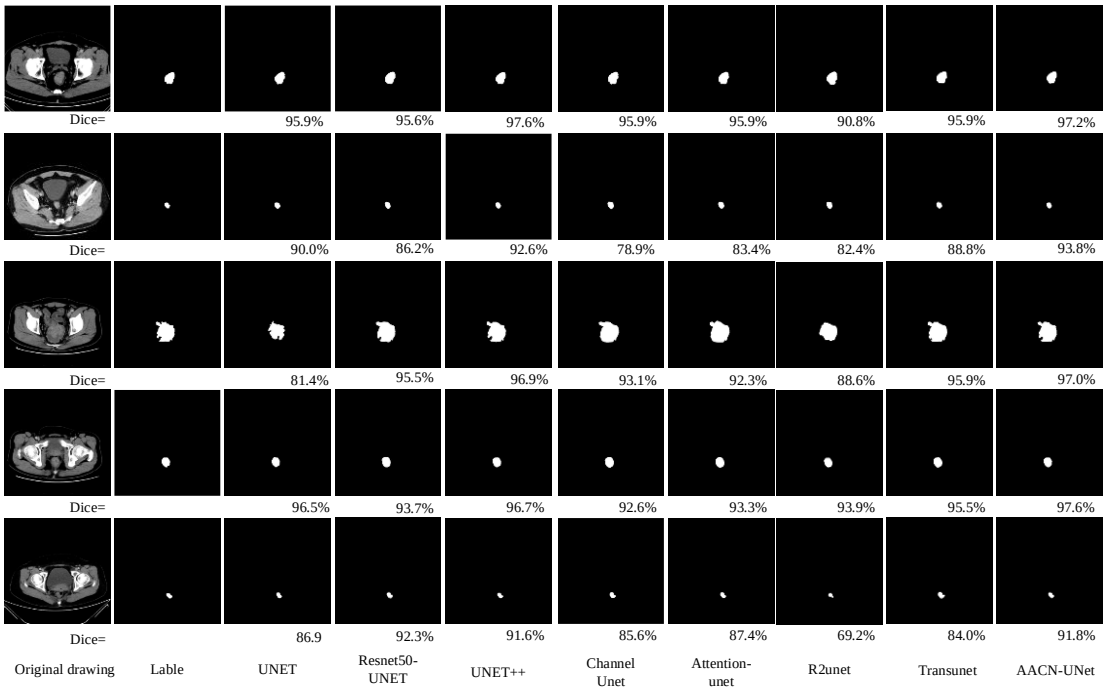

Figure 8.Test set verification results of different networks

Therefore, in this paper, the spatial attention module and the channel attention module in the spatial CBAM are taken out separately, the spatial attention module and the ConvNeXt UNet model are combined as SCAN-UNet (Spatial Attention ConvNeXt UNet), and the channel attention module and the ConvNeXt UNet model are combined as CACN-UNet (Channel Attention ConvNeXt UNet), and the comparative experiments are conducted with AACN-UNet.

Table 4.Rectal cancer tumour segmentation results using different attention mechanisms

Module	P	R	F-score	Iou
SACN-UNet	93.9	93.4	93.6	88.6
CACN-UNet	94.0	94.5	94.5	89.6
AACN-UNet	**95.0**	**95.3**	**95.1**	**91.5**
CN-UNet	93.8	93.7	93.4	88.8

The experimental results are shown in Table 3. From table 3, it can be seen that compared with SACN-UNet, AACN-UNet has increased P, R, F1 and Iou by 1.1%, 1.9%, 1.5% and 2.9% respectively. Compared with CACN-UNet, the P, R, F1 and Iou of AACN-UNET increased by 1.0%, 0.8%, 1.1% and 1.9% respectively. Therefore, the evaluation indexes of AACN-UNet are better than those of SACN-UNet and CACN-UNet, which shows that the CBAM attention module combining spatial attention and channel attention can improve the segmentation performance very well.

In order to have a better understanding of the attention module, this paper uses the Grad-Cam to visualize the last up sampled attention module in AACN-UNet, as shown in the figure below. The calculation of the model focuses on the rectal tumour.

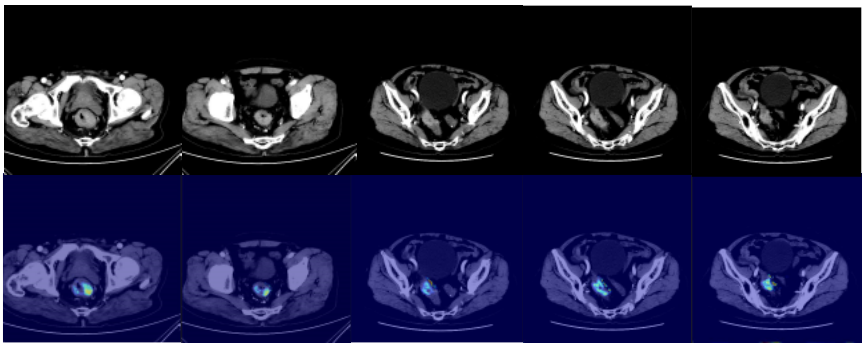

Figure 9.Test set verification results of different networks

5. Conclusion

Rectal cancer is one of the most serious malignant tumours in the world, with high mortality. Accurate segmentation of rectal tumour region is the key to early diagnosis of rectal cancer. The AACN-UNet proposed in this paper is a highlight in rectal cancer tumour segmentation. The network backbone feature extraction network uses ConvNeXt network and CBAM attention mechanism to embed it into the network. The experimental results show that the rectal tumour segmentation network proposed in this paper can achieve the most advanced rectal tumour segmentation performance, while reducing the network complexity and training time. The proposed network helps to reduce the labor intensity of doctors, timely treat diseases for patients, and save valuable time.

Because of the value of medical image resources, this paper only trains and tests the proposed segmentation network model in a small database. In the future, we hope to collect more rectal tumour images, expand the database, and improve the model accuracy. At the same time, we hope to further train and test the model in other medical CT image databases, so as to further display its performance.

Acknowledgments

Disclosure statement

References

Alom MZ, Hasan M, Yakopcic C, Taha, TM, & Asari VK. 2018. Recurrent residual convolutional neural network based on u-net (r2u-net) for medical image segmentation.

Cao H, Wang Y, Chen J, Jiang D, Zhang X, & Tian Q, et al. 2021. Swin-unet: unet-like pure transformer for medical image segmentation.

Chen Y, Wang K, Liao X, Qian Y, & Heng PA. 2019. Channel-unet: a spatial channel-wise convolutional neural network for liver and tumours segmentation. Frontiers in Genetics, 10, 1110.

Chen J, Lu Y, Yu Q, Luo X, & Zhou Y. 2021. Transunet: transformers make strong encoders for medical image segmentation.

Desantis CE, Lin CC, Mariotto AB, Siegel RL, Stein KD, & Kramer JL, et al. 2013. Cancer treatment and survivorship statistics, 2014.

Fu J, Liu J, Tian H, Li Y, Bao Y, & Fang Z, et al. 2020. Dual Attention Network for Scene Segmentation. 2019 IEEE/CVF Conference on Computer Vision and Pattern Recognition (CVPR). IEEE.

Green B, Bogart A, Chubak J, Vernon S, & Wang CY. 2011. C-c3-05: characteristics of patients not up-to-date for colorectal cancer screening (crcs) and who decline participation in a trial to increase screening. Clinical Medicine & Research, 9(3-4), 142.

Howard AG, Zhu M, Chen B, Kalenichenko D, Wang W, & Weyand T, et al. 2017. Mobilenets: efficient convolutional neural networks for mobile vision applications.

Jie H, Li S, Gang S, & Albanie S. 2017. Squeeze-and-excitation networks. IEEE Transactions on Pattern Analysis and Machine Intelligence, PP(99).

Li X, Wang W, Hu X, & Yang, J. 2020. Selective Kernel Networks. 2019 IEEE/CVF Conference on Computer Vision and Pattern Recognition (CVPR). IEEE.

Liu Z, Lin Y, Cao Y, Hu H, Wei Y, & Zhang Z, et al. 2021. Swin transformer: hierarchical vision transformer using shifted windows.

Liu Z, Mao H, Wu CY, Feichtenhofer C, Darrell T, & Xie S. 2022. A convnet for the 2020s. arXiv e-prints.

Oktay O, Schlemper J, Folgoc LL, Lee M, Heinrich M, & Misawa K, et al. 2018. Attention u-net: learning where to look for the pancreas.

O Ronneberger, P Fischer and T Brox. 2015 U-Net: Convolutional Networks for Biomedical Image Segmentation. In Proceedings of the Medical Image Computing and Computer-Assisted Intervention, pp.234-241.

Siegel RL, Miller KD, Sauer AG, Fedewa SA, Butterly LF, & Anderson JC, et al. 2020. Colorectal cancer statistics, 2020. CA: A Cancer Journal for Clinicians, 70.

S. Woo, J. Park, J.-Y. Lee, and I. S. Kweon, "Cbam: Convolutional block attention module," in Proceedings of the European conference on computer vision (ECCV), 2018, pp. 3–19

Trebing K, T Stańczyk, & Mehrkanoon S. (2021). Smaat-unet: precipitation nowcasting using a small attention-unet architecture. Pattern Recognition Letters, 145, 178-186.

Vaswani A, Shazeer N, Parmar N, Uszkoreit J, Jones L, & Gomez A N, et al. 2017. Attention Is All You Need. arXiv. arXiv.

Xie S, Girshick R, P Dollár, Tu Z, & He K. 2016. Aggregated residual transformations for deep neural networks. IEEE.

Yeung M, Sala E, Schnlieb CB, & Rundo L. 2021. Generalised focal loss: unifying dice and cross entropy-based losses to handle class imbalanced medical image segmentation.

Zhang Z, & Sabuncu, M. R. 2018. Generalized cross entropy loss for training deep neural networks with noisy labels.

Zhou Z, Siddiquee MMR, Tajbakhsh N, & Liang J. 2018. Unet++: a nested u-ne t architecture for medical image segmentation.

The Seven Teddy Cup Mining Challenge Comprtition. http://www.tipdm.org/u/cms/www/201903/15214944i2k3.pdf. Rectal cancer dataset [EB/OL].

中国结直肠癌筛查与早诊早治指南(2020).[Guidelines for screening and early diagnosis and treatment of colorectal cancer in China(2020)] .Beijing.1-28.Chinese.